Journal of University of Science and Technology Beijing
Volume 11, Number 1, February 2004, Page 13

Metallurgy

3-D transient numerical simulation on the process of laser cladding by powder feeding

Yanlu Huang, Gongying Liang, and Junyi Su

School of Materials Science and Engineering, Xi'an Jiaotong University, Xi'an 710049, China
(Received 2003-04-11)

Abstract: A 3-D transient mathematical model for laser cladding by powder feeding was developed to examine the macroscopic heat and momentum transport during the process, based on which a novel method for determining the configuration and thickness of cladding layer was presented. By using Lambert-Beer theorem and Mie's theory, the interaction between powder stream and laser beam was treated to evoke their subtle effects on heat transfer and fluid flow in laser molten pool. The numerical study was performed in a co-ordinate system moving with the laser at a constant scanning speed. A fixed grid enthalpy-porosity approach was used, which predicted the evolutionary development of the laser molten pool. The commercial software PHOENICS, to which several modules were appended, was used to accomplish the simulation. The results obtained by the simulation were coincident with those measured in experiment basically.

Key words: powder feeding; laser cladding; numerical simulation; cladding track; heat transfer

[*This work was financially supported by the National Natural Science Foundation of China (No. 50271051) and the Foundation of State Key Laboratory of Laser Technology, Huazhong University of Science and Technology.*]

1 Introduction

Laser cladding process is rather complicated and hard to control due to the multitude of process parameters involved, and the temperature field of the heat affected zone is difficult to measure due to the rapid fusion and solidification. Thus the numerical simulation method has gotten flourishing in researches on laser cladding. In laser cladding by powder feeding, the interaction between powder stream and laser beam and the configuration of the cladding layer are important factors affecting the whole temperature field and the final quality of laser cladding. But in previous models [1-4], the configuration of the cladding layer was treated by either experiences or shortcut calculations. And these models took no account of the interaction between powder stream and laser beam. As a matter of fact, the interaction between powder stream and laser beam changes the laser intensity distribution and the particle temperature distribution when they reach the laser molten pool. The aim of the present work is to develop a comprehensive 3-dimensional numerical model for most important physical phenomena during laser cladding, such as the fluid flow and heat transfer in molten pool, the interaction between powder stream and laser beam and the formation of the cladding layer and so on.

2 Physical model

Figure 1 shows schematic diagram of a laser cladding process. A laser beam moving with a constant scanning speed in the horizontal direction and a part of energy is absorbed. A thin melt pool forms on the surface due to laser heating. Simultaneously, a powder stream of a different material is fed into the pool. As the laser source moves away from a location, resolidification of the zone occurs, forming to a final cladding layer. The laser beam and the powder stream interact with each other over the workpiece so that the laser power is partially attenuated and the powder is heated by laser beam.

The interactions among laser beam, powder stream and the specimen are very complex, so some assumptions are made in formulation of the model:

(1) The origin of coordinates is located at the center of the laser beam;

(2) The powder particles are spherical;

(3) The liquid metal is incompressible Newtonian

Corresponding author: Yanlu Huang, **E-mail:** ylyellow@163.net

fluid, and the flow in molten pool is laminar;

(4) The driving forces of the flow in molten pool are buoyancy and surface tension gradient due to temperature difference, and the velocity in solid equals to zero;

(5) Only the powders entering into the molten pool are formed into cladding layer, other powders rebounding from the solid surface are lost.

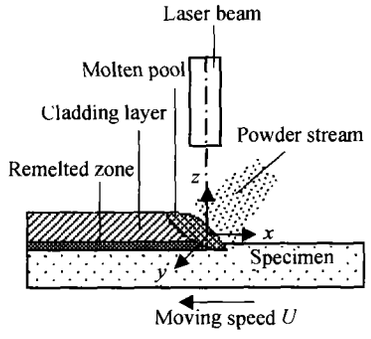

Figure 1 Schematic diagram of the laser cladding process.

3 Mathematical and numerical model

Fluid flow and heat transfer in molten pool, interaction between laser beam and powder stream and the formation of the cladding layer are the most important physical processes. The mathematical model for such processes is expatiated below.

3.1 Solution of the velocity and temperature fields

The continuum model for binary solid-liquid phase change system [5] was used, and a fixed-grid and moving coordinate system was adopted to deal with fluid flow and heat transfer problem involving moving heat source.

(1) Governing equations of fluid flow.

Continuity equation

$$\frac{\partial \rho}{\partial t}+\frac{\partial(\rho u_j)}{\partial x_j}=0 \tag{1}$$

Momentum equation

$$\frac{\partial(\rho u_i)}{\partial t}+\frac{\partial(\rho u_i u_j)}{\partial x_j}=\frac{\partial}{\partial x_j}\left(\mu\frac{\partial u_i}{\partial x_j}\right)-\frac{\partial p}{\partial x_i}+S_i \tag{2}$$

where ρ is the density, t the time, u_j the average velocity in x_j direction: $u_j=f_l u_{jl}$, f_l the liquid mass fraction, u_{jl} the liquid velocity in x_j direction; μ the dynamic viscosity; p the pressure and S_i the source term as follows:

$$S_i=-\frac{\mu}{K}\frac{\rho}{\rho_l}u_i+\frac{\partial(\rho U_i u_i)}{\partial x_i}+\rho_{ref}g_i\beta(T-T_{ref}) \tag{3}$$

where the first term is Darcy's term and K is osmotic coefficient which is defined by Carmon-Kozeny equation [6]:

$$K=K_0\frac{f_l^3}{(1-f_l)^2} \tag{4}$$

where K_0 is a constant connecting with the appearance of the media; the second term is the additional convection term due to the sample movement and U_i is the sample velocity in x_i direction; the third term is the buoyancy due to temperature difference and T is the temperature, T_{ref} the reference temperature, ρ_{ref} the density at T_{ref} and g_i the acceleration of gravity in x_i direction.

The boundary condition of the momentum equation is as below:

$$\mu\left(\frac{\partial v}{\partial l}\right)_n=-f_l\left(\frac{\mathrm{d}\gamma}{\mathrm{d}T}\frac{\mathrm{d}T}{\mathrm{d}l}\right)_\tau \tag{5}$$

where v is the velocity, $\frac{\mathrm{d}\gamma}{\mathrm{d}T}$ the surface tension coefficient, $\frac{\mathrm{d}T}{\mathrm{d}l}$ the temperature gradient, l the distance, where the subscript n and τ denote the normal direction and tangential direction, respectively.

(2) Governing equation of heat transfer.

The energy conservation equation expressed by sensible enthalpy h is:

$$\frac{\partial(\rho h)}{\partial t}+\frac{\partial(\rho u_i h)}{\partial x_i}=\frac{\partial}{\partial x_i}\left(\frac{k}{c}\frac{\partial h}{\partial x_i}\right)+S_h \tag{6}$$

where k is the mixture average conductivity, and c the mixture average specific heat capacity, S_h the global source term just as below:

$$S_h=q+\left[\frac{\partial(\rho\Delta H)}{\partial t}+\frac{\partial(\rho u_i\Delta H)}{\partial x_i}\right]+\frac{\partial}{\partial x}[\rho U_i(h+\Delta H)] \tag{7}$$

where the first term is the heat entering into the molten pool with powders, the second the transient and convection terms of the latent heat and the third the heat transfer due to the sample movement including the sensible enthalpy term and latent heat one. ΔH is a function of temperature expressed as follows:

$$\Delta H=\begin{cases}L & T\geq T_l\\ Lf_l & T_s<T<T_l\\ 0 & T\leq T_s\end{cases} \tag{8}$$

where L is the latent heat, T_s and T_l the solidus and the liquids temperature, respectively.

The laser intensity $Q(r)$ with gaussian distribution

is the boundary condition of the energy conservation equation:

$$Q(r)=\frac{3P}{\pi R^2}\exp\left(-\frac{3r^2}{R^2}\right) \tag{9}$$

where r is the distance from the center of the laser beam, P the laser power and R the effective radii of the laser beam.

For each surface of the sample, there exists a heat exchange with environment.

3.2 Flag variable method

The formation of cladding layer is conditional on the powders entering into the molten pool and the sample movement. Here a flag variable F is defined to denote the state of every cell: 1 the cladding layer cell, 0 the empty cell and 0~1 the surface cell; F values are refreshed at the end of each step according to the following formula:

$$\begin{cases} F_k^{t+\Delta t}=(M_T-M_L^K)/(\rho_{cl}\cdot V_c) \\ F_k^{t+\Delta t}=\max(F_k^{t+\Delta t},0) \\ F_k^{t+\Delta t}=\min(1,F_k^{t+\Delta t}) \end{cases} \tag{10}$$

where M_T is the total mass of the cladding in a vertical column of cells, M_L^k the total mass below the surface cell, ρ_{cl} the cladding density and V_c the current cell volume.

The deformation of the cladding layer due to the sample movement, fluid flow in molten pool and the powder feeding at the end of each step can be described as follows:

$$\frac{\partial(\rho F)}{\partial t}+\frac{\partial(\rho U_i F)}{\partial x_i}+\frac{\partial(\rho u_i F)}{\partial x_i}=m \tag{11}$$

where m is the powder feeding rate, using $F'^{(t+\Delta t)}$ obtained by the above equation, the total mass M_T can be calculated:

$$M_T=\sum(\rho_{cl}F'^{(t+\Delta t)}V_c) \tag{12}$$

For any k cell in any column, M_L is calculated by the following formula:

$$M_L^k=\sum_{z=1}^{k-1}(\rho_{cl}F_z^{t+\Delta t}V_c) \tag{13}$$

Then $F_z^{t+\Delta t}$ can be calculated by the following computational procedure:

(a) Initially $M_L^1=0$, $F_1^{t+\Delta t}$ can be calculated by equation (10);

(b) Using $F_1^{t+\Delta t}$, M_L^2 can be calculated by equation (13);

(c) Using M_L^2, $F_2^{t+\Delta t}$ can be calculated by equation (10);

(d) Using $F_1^{t+\Delta t}$ and $F_2^{t+\Delta t}$, M_L^3 can be calculated by equation (13), then $F_3^{t+\Delta t}$ is calculated by equation (10).

An updated clear cladding configuration at the end of the current step can be obtained when all F values are updated according to the above procedure.

3.3 Interaction between laser beam and powder stream

The interaction between laser beam and powder stream leads to attenuation of laser and makes the powder temperatures raise. An analytical model is presented below to study the temperature distribution of the powders and their attenuation on laser energy distribution.

According to the Lambert-Beer theorem and Mie's theory [7,8], the laser power through the powder stream is attenuated exponentially:

$$Q'_1(r,l)=Q(r)\cdot\exp(-\sigma_{ext}Nl) \tag{14}$$

where $Q'_1(r,l)$ is the laser intensity at r from the laser beam center after traveling a distance l in powder stream, σ_{ext} the extinction area and N the powder concentration in the stream. In this paper the attenuation of the laser powder is calculated layer by layer along z-direction, the initial value of $Q(r)$ is derived from formula (9).

The temperature increment of the spherical particle traveling a certain distance in laser beam can be calculated by the following formula:

$$Q'_1(r,l)\cdot\alpha_p\cdot 2\pi r_p^2\cdot\frac{s}{v_p}=\rho_p\cdot\frac{4}{3}\pi r_p^3\cdot c_p\cdot\Delta T \tag{15}$$

where α_p is the laser absorptivity of the powder, r_P the average radii, s the traveling distance in laser beam, v_P the traveling speed, ρ_p the density, c_P the specific heat capacity and ΔT the temperature increment. In this paper the temperature increment is calculated layer by layer along the x-direction, s is the current Δx and v_P the x- component of the actual velocity.

3.4 Numerical simulation

Since continuum model has been adopted, explicit tracking of internal boundaries among solid, liquid and mushy regions are unnecessary. Hence, fixed grid system is used in the numerical scheme. The governing equations are discretized using the control-volume-based finite-difference approach, with an upwind scheme for the convective terms. SIMPLEST algorithm is adopted to resolve the velocity-pressure

coupling in the momentum equations. Iteration solution is adopted to account for the coupling among the various equations. At each time-step, the velocity field is computed first, using the previously computed liquid fraction, permeability and physical parameters. Then, temperature is calculated. Next, the liquid fraction is updated based on computed temperature, permeability and physical parameters are updated according to the liquid fraction, and this process is repeated up to obtaining convergence solution.

4 Experimental verification of numerical simulation

4.1 Experimental

A series of work has been done by Frenk *et al.* [3] to measure the cladding thickness and the molten pool shape. In these experiments, the laser power was 1380W, the laser spot radii was 2.0 mm; the cladding material was stellite6 alloy, the substrate material was 0.08% mild steel, the sample size is 25 mm×10 mm× 10 mm.

The simulation is accomplished through appending some modules to the commercial software PHOENICS. The parameters used are below [2]: for stellite6 alloy, density 8400 kg/m^3, solid conductivity $(13.39+0.028T)$ W·(°C·m)$^{-1}$, liquid conductivity 48.8W·(°C·m)$^{-1}$, specific heat capacity 416.7 J·(°C·kg)$^{-1}$, fusion heat (3.1×10^5) J/kg, kinematic viscosity (7.1×10^{-7})m^2/s, liquidus temperature 1354°C, solidus temperature 1265°C, liquid expansion coefficient 1.33×10^{-4}, laser absorptivity 31%; for mild steel, density 7800 kg/m^3, solid conductivity $(65.0-0.05T+2\times10^{-5}T^2)$ W·(°C·m)$^{-1}$, liquid conductivity 35 W·(°C·m)$^{-1}$, specific heat capacity 610 J·(°C·kg)$^{-1}$, fusion heat (2.46×10^5) J/kg, liquidus temperature 1530°C, solidus temperature 1493°C.

4.2 Comparison of computed and experimental results

Two experiments were simulated in this paper. For the first one the scanning velocity and the powder feeding rate were 8.33 mm/s and 0.067 g/s, respectively, and 20 mm/s and 0.15 g/s for the second one. The cladding configuration, the development of the molten pool and the flow field obtained by simulation are shown in **figure 2**. It can be seen that the steady stage begins after 0.5 s for the first experiment, and 0.15 s for the second, and that the cladding layer has a curved surface, the supposition of a flat surface or a spherical one differs from the reality. To further illuminate a steady laser cladding process, **figure 3** shows the 3-dimensional sketch of the cladding layer and the laser molten pool for the second experiment at the time 0.4 s, the velocity field of the liquid zone and the mushy zone is also plotted in figure 3. The computed and experimental results are compared in **table 1**, H_c is the cladding thickness, L_M and W_M are the length and width of horizontal projection of the molten pool. The computed results coincide with the experimental ones.

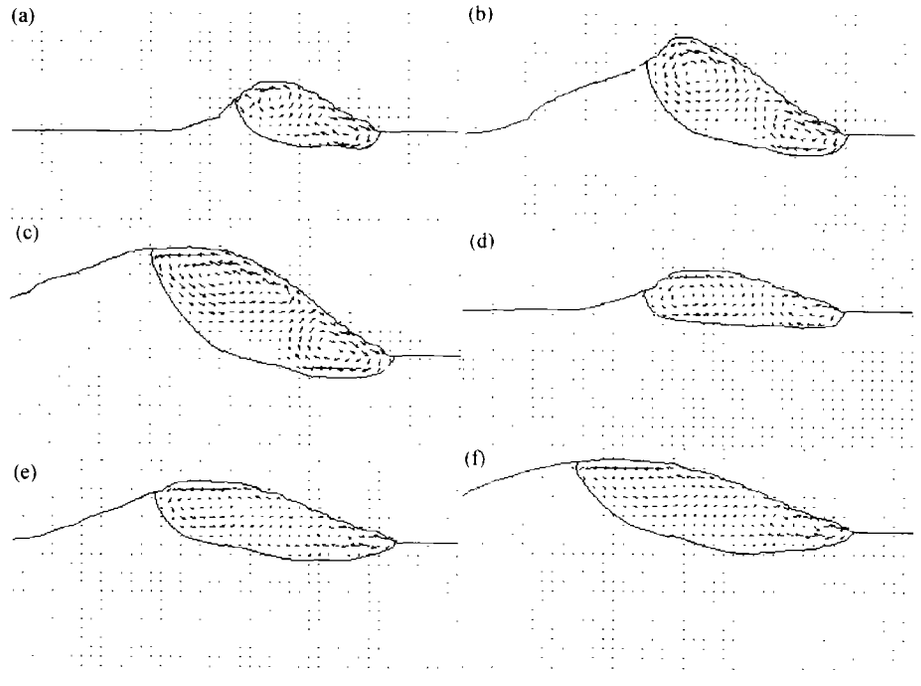

Figure 2 Development of the cladding layer, the shape of molten pool and fluid flow, (a) experiment 1, 0.1 s; (b) experiment 1, 0.3 s; (c) experiment 1, 0.5 s; (d) experiment 2, 0.05 s; (e) experiment 2, 0.1 s; (f) experiment 2, 0.15 s.

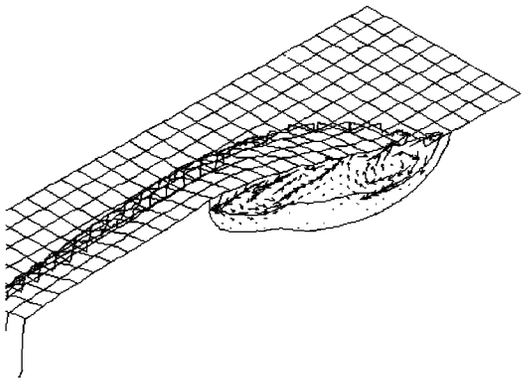

Figure 3 3-D sketch of a steady laser cladding process at the viewpoint of (1, 1, 1).

Table 1 Comparison of H_c, L_M and W_M

No.	Experiments	H_C / mm	L_M / mm	W_M / mm
1	Experimental data	0.73	1.72	1.68
	Computed data	0.77	1.81	1.73
2	Experimental data	0.63	1.72	1.55
	Computed tata	0.68	1.82	1.62

5 Conclusions

(1) A continuum model was adopted to deal with the transport phenomena of the solid-liquid phase change system in a co-ordinate system moving with the laser, the coupled simulation of the velocity and temperature fields were carried out by using controlled-volume finite difference method.

(2) A novel method for computing the formation of the cladding layer was presented.

(3) Using Lambert-Beer theorem and Mie's theory, the interaction between laser beam and powder stream was calculated to evoke their subtle effects on the dynamic process in laser molten pool.

(4) The computed results were coincident with those obtained in the experiments.

References

[1] B. Ollier, N. Pirch, and E.W. Kreutz, A numerical model of the one-step laser cladding process [J], *Laser Photons*, 1(1996), No.1, p.8.

[2] A.F.A. Hoadley and M. Rappaz, A thermal model of laser cladding by powder injection [J], *Metall. Trans.*, 23B(1992), p.631.

[3] A. Frenk, M. Vandyoussefi, and J.D. Wagniere, *et al.*, Analysis of the laser-cladding process for stellite on steel [J], *Metall. Mater. Trans.*, 28B(1997), p.501.

[4] Dawen Zeng and Changsheng Xie, A numerical simulation for two dimensional quasi-state fluid flow field and temperature field in the molten pool of laser cladding [J], *Acta Metall. Sin.* (in Chinese), 35(1999), No.6, p.604.

[5] W.D. Bennon and F.P. Incropera, A continuum model for momentum, heat and specics transport in binary solid-liquid phase change systems (I. model formulation) [J], *Int. J. Heat Mass Transfer*, 30(1987), No.6, p.2162.

[6] P.G. Sismanis and S.A. Argyropoulos, Modeling of exothermic dissolution [J], *Can. Metall. Q.*, 27(1988), No.2, p.123.

[7] M. Born and E. Wolf, *Principles of Optics: electromagnetic theory of propagation, interference and diffraction of light* [M] (in Chinese), Science Press, Beijing, 1978.

[8] M. Kerker, *The Scattering of Light and Electromagnetic Radiation* [M], Academic Press, New York, 1969.